PHYSICAL REVIEW B

CONDENSED MATTER

THIRD SERIES, VOLUME 43, NUMBER 12 15 APRIL 1991-II

Local adsorbate-induced effects on dynamical charge transfer in ion-surface interactions

G. A. Kimmel, D. M. Goodstein,* Z. H. Levine,† and B. H. Cooper

Laboratory of Atomic and Solid State Physics, Cornell University, Ithaca, New York 14853-2501

(Received 19 September 1990; revised manuscript received 10 December 1990)

We have measured positive-ion survival probabilities for K^+ scattered from clean and alkali-metal-adsorbate-covered Cu(100) and Cu(110). As expected from most models of resonant charge transfer, we find that very small coverages of alkali-metal adsorbates on the surface can dramatically decrease the ion survival probability. However, the dependence of the ion survival probability on adsorbate coverage is qualitatively different from that expected on the basis of the adsorbate-induced work-function change. We find that a treatment of the charge transfer based on the spinless Newns-Anderson Hamiltonian explains the data only if the local electrostatic potential of the adsorbate overlayer is included in the calculations.

I. INTRODUCTION

Resonant charge transfer (i.e., the exchange of electrons between states of equal energy) plays an essential role in a number of dynamical processes that involve the interactions of atoms and molecules with surfaces, such as molecular dissociation and chemisorption. Ion-surface charge transfer is also important in secondary-ion mass spectroscopy (SIMS), where knowledge of absolute neutralization rates is essential for quantitative analysis. Because they are of such fundamental importance in particle-surface interactions, considerable theoretical and experimental effort has been devoted to the study of charge-transfer mechanisms at surfaces.[1–14] A comprehensive listing of references may be found in recent review articles on both experimental[15] and theoretical[16] work in this area.

Details of the charge-transfer process depend directly on both the energies of the atomic or molecular states and their couplings to the metallic states. Thus it is not surprising that charge-transfer rates can be sensitive to changes in the surface electronic structure.[4,6] For example, the presence of even small coverages of adsorbates can change charge-transfer rates significantly.[11–13] In some cases, the effect of electropositive or electronegative adsorbates on charge-transfer processes may be important in influencing surface reaction rates.[17] Our objective here is to investigate, under controlled conditions, how the charge-transfer process depends on the presence of adsorbates and, in particular, the inhomogeneous electrostatic potential induced by the adsorbates. Theoretical calculations have investigated the related issue of the role of the local electrostatic potential of adsorbates in the poisoning and promotion of surface catalytic reactions.[18,19] The variation of the local electrostatic potential around alkali-metal adsorbates has also been investigated experimentally using photoemission of adsorbed xenon (PAX)[20] and metastable-He deexcitation spectroscopy (MDS).[21–24]

The effect of adsorbates on the neutralization of scattered or sputtered atoms has been considered explicitly in several studies.[11–14,25] It has been known for some time that charge-transfer rates are very sensitive to adsorbate-induced shifts in the work function. While inclusion of the work-function shift reproduces general features of the experimentally observed behavior, it was suggested by Brako and Newns[4] that neutralization of alkali-metal ions could be locally enhanced at individual electropositive adsorbate sites. A recent ion-scattering study by Geerlings *et al.*[12] has shown that, in order to reproduce the observed dependence of the charge-transfer rate on adsorbate coverage, it is necessary to consider local effects such as inhomogeneities in the electrostatic potential around individual adsorbate sites. In that analysis, one type of scattering trajectory was considered: glacing-angle collisions with adsorbate atoms.

We have extended these concepts to a more general trajectory-dependent analysis of charge transfer from adsorbate-covered surfaces. Positive-ion survival probabilities were measured for low and hyperthermal energy K^+ scattered from clean and alkali-metal-adsorbate-covered Cu(100) and Cu(110).[13] We apply a model of resonant charge transfer to our data which includes the local electrostatic potential of the adsorbates. Features in the experimental energy spectra are unambiguously assigned to specific ion trajectories with the aid of the

SAFARI computer simulation, giving us detailed knowledge of the history of the ion's interaction with the surface.[26] A simple model of the adsorbate overlayer is used to calculate the electrostatic potential along an appropriate atom-scattering trajectory generated by SAFARI. The energy of the atom's ionization level and its coupling to the metallic states are used to find its occupancy as a function of position along the trajectory. The parameters used in the model were obtained either experimentally or from theoretical calculations. The model gives good qualitative agreement and reasonable quantitative agreement with the data and clearly supports the conclusion that the local electrostatic potential of adsorbates can be important in the charge-transfer process.

Section II discusses the standard model of resonant charge transfer for alkali-metal ions interacting with metal surfaces. Section III gives details of the equipment and experimental procedure. Section IV compares the data and the standard model. Section V discusses a model which treats the case of scattering from adsorbate-covered surfaces. In Sec. VI this model is further discussed and compared to data for scattering at different energies and geometries. The last section summarizes the results.

II. REVIEW OF THE THEORY OF RESONANT CHARGE TRANSFER

In this section, we will briefly review the standard theoretical treatment of resonant charge transfer on which we base our model. In the standard treatment the sole effect of an adsorbate layer is to shift the work function. We will show in Sec. IV that this fails to quantitatively reproduce our data and in Secs. V and VI discuss what changes we have made to treat the case of scattering from adsorbate-covered surfaces.

Resonant charge transfer involves the exchange of an electron between states in the metal and an atomic state at the same energy. The adiabatic charge distribution for an atom-metal (or molecule-metal) system is determined by the relative energies of the various electronic levels. Since the energies of levels in atoms and molecules change as they approach or leave a surface, their adiabatic occupation may also change. The occupation of the level depends on its energy (relative to the Fermi energy), which varies with distance due to the interaction of the atom with the surface. When the atom is close to the surface ($z \sim 1$ Å), the lifetimes of the atomic levels are short compared with the atom-surface interaction time for the scattering energies of interest here. As the atom leaves the surface, the coupling of the atomic and metallic states decreases (roughly exponentially) with distance, and the lifetime of the state becomes long compared with the interaction time. Thus, the finite velocity of the particles can lead to nonadiabatic effects in the charge-transfer process.

We first consider the energetics of charge transfer. Consider two states of the alkali-metal system, one in which the atom and metal are neutral ($A+M$), and another in which the atom is positively ionized and the metal is negatively charged ($A^+ + M^-$). Assume that the atom is in its electronic ground state and that the metal has no electron-hole excitations. Figure 1(a) schematically represents the variation of the diabatic total-energy curves for the neutral and singly ionized systems.[6,8] The neutral atom experiences long-range van der Waals forces when it is far from the surface and a strong Pauli repulsion very close the surface. For the ion, the dominant interaction at large distances will be the electrostatic attraction of the ion and its image charge, which is much stronger than the van der Waals interaction. Very close to the surface, the ion will also be strongly repulsed.

For alkali metals interacting with a high-work-function metal surface, we assume that only a single atomic orbital (the first ionization level) is likely to be involved in the charge transfer. At very large distances from the surface, the energy difference between the two states ($A^+ + M^-$ and $A+M$) is the first ionization potential I minus the work function Φ of the metal. (Assume that the system is closed.) If the ionization level of the atom is larger than

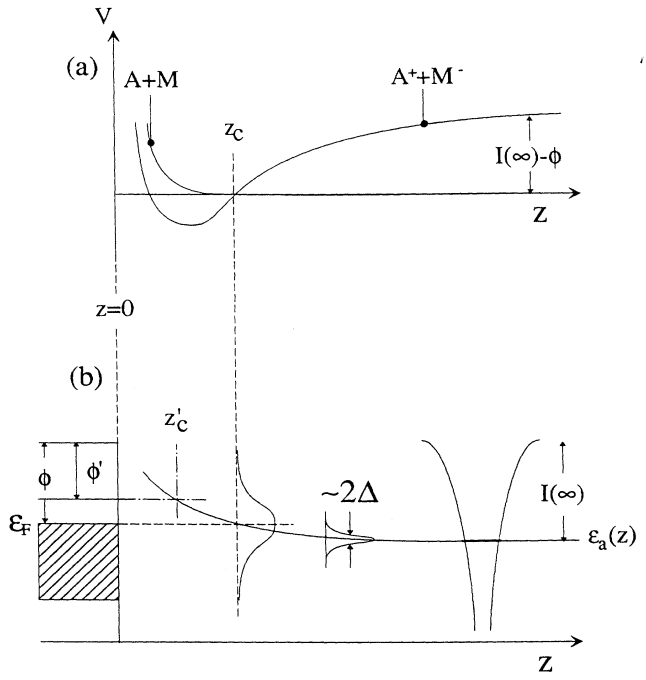

FIG. 1. Schematic representations of the interaction of an atom with a metal surface. (a) Diabatic, total potential energy vs distance for a neutral atom ($A+M$) and an ion ($A^+ + M^-$) interacting with a metal. The variation, for large z, in the $A^+ + M^-$ system is due to the attraction of the ion with its image charge. A level crossing can occur, $z = z_c$, if at $z = \infty$, $I > \Phi$, where I is the first ionization energy of the atom and Φ is the work function. (b) By taking the difference between the $A+M$ and $A^+ + M^-$ curves, we obtain the variation of the ionization level with distance from the surface [$\varepsilon_a(z)$]. The lifetime of the level is inversely proportional to the level width Δ. For $z < z_c$ ($> z_c$), it is energetically favorable for the level to be empty (full). Changing the work function of the surface (Φ') changes the level crossing distance (z_c') and thus changes the ion survival probability.

the work function [as in Fig. 1(a)], then at some distance z_c outside the surface, the two diabatic curves may be degenerate.

In a one-electron picture,[27,28] a level crossing occurs ($z=z_c$) when the ionization level is degenerate with the Fermi level [Fig. 1(b)]. For the relevant separations of interest here, the variation in energy of the first ionization level with distance outside the surface $\varepsilon_a(z)$ is due to the image interaction and is found by taking the difference between the $A^+ + M^-$ and $A + M$ diabatic curves in Fig. 1(a).[8] Thus $\varepsilon_a(z)$ (Ref. 29) is given by (all equations are in atomic units)

$$\varepsilon_a(z) = -I + \frac{1}{4(z - z_{\rm im})} , \tag{1}$$

where $z_{\rm im}$ is the location of the image plane.[30] The level crossing occurs when $\varepsilon_a(z_c) = -\Phi$.

At the level-crossing distance z_c, an electron can transfer from the Fermi level in the metal to the atomic ionization level (or vice versa) leaving the metal in its ground state. At distances greater than z_c, an electron from below the Fermi level can transfer to the atomic ionization level, leaving the metal in an excited state.[31] Similarly for $z < z_c$, the atom can transfer an electron to a state above the Fermi level, again leaving the metal in an excited state.

A model of resonant charge transfer, based on the spinless Newns-Anderson Hamiltonian, has been developed to treat the case of atoms or molecules scattered or sputtered from metal surfaces.[1,4,5] Variations of this model have been used successfully to describe the neutralization of Cs atoms sputtered from an Al substrate,[11] the formation of O^- sputtered from V,[5] and the neutralization of Na scattered from W.[4]

Within this model, to calculate the charge-transfer probability, one needs to solve the time-dependent Schrödinger equation for the discrete atomic level interacting with a continuum. For the case of ion scattering or sputtering, certain simplifying assumptions are often made. It is assumed that the ion has a constant velocity after leaving the surface. Furthermore, the atomic energy level ε_a and the coupling Δ are assumed to depend only on the distance of the ion from the surface. $\varepsilon_a(z)$ is assumed to decrease monotonically as z increases [see Eq. (1)]. Since $\Delta(z)$ is related to the overlap of the atomic and metallic orbitals which are exponentially decaying, it is usually assumed to be of the form

$$\Delta(z) = \Delta_0 e^{-\alpha z} . \tag{2}$$

With these assumptions, the ion survival probability P^+ is given by[4,5]

$$P^+ = \exp\left[\frac{-2\Delta(z_c)}{\alpha v_z} \right] , \tag{3}$$

where v_z is the component of the final velocity perpendicular to the surface. Using Eqs. (1)–(3) the ion survival probability versus work function is

$$P^+ = \exp\left[\frac{-2\Delta_0}{\alpha v_z} e^{-\alpha z_{\rm im}} \exp\frac{-\alpha}{4(I-\Phi)} \right] . \tag{4}$$

Since the ion-survival probability depends exponentially on the coupling strength in the region of the level crossing [see Eq. (3)], changing the level-crossing distance z_c provides a method for testing this model. The level crossing can be changed by varying the work function Φ of the metal. When the work function is larger than the ionization potential ($\Phi > I$), as for K^+ scattering from clean Cu(100) or Cu(110), no level crossing occurs ($z_c = \infty$) and the ion-survival probability is one. For $\Phi < I$, the ion-survival probability decreases rapidly as the work function and z_c both decrease. The effect of changing the work function is shown schematically in Fig. 1. This is achieved experimentally by the adsorption of various overlayers.

Previous experiments have measured the ion-survival probability of scattered or sputtered atoms versus the work function.[10–13] For example, Yu measured the yield of cesium ions sputtered from several different substrates (Au, Al, and Si) where different coverages of adsorbed lithium were used to vary the work function.[11] Figure 2 shows results for Cs^+ sputtered from Li/Al along with the predictions of Eq. (4). The parameters for the fit were obtained from calculations by Lang.[11] The data are well reproduced by Eq. (4). In particular, the plateau in the ion yield for $\Phi > I$ and the rapid decrease for $\Phi < I$ are seen.

III. EXPERIMENTAL PROCEDURE

The experimental apparatus and procedures have been described elsewhere,[32] so only a brief outline will be given here. The experiments were performed in an ultrahigh-vacuum (UHV) system with a base pressure of 1×10^{-10} Torr. Well-collimated and monochromatic K^+-ion beams with energies from 100 to 1000 eV were used in

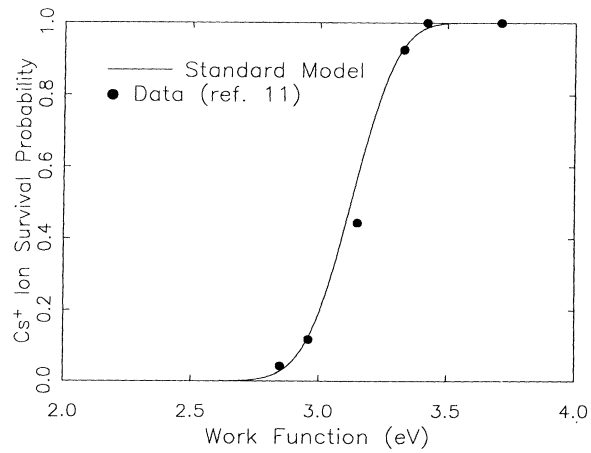

FIG. 2. Yu's results for the ion survival probability vs work function of Cs sputtered from an Al substrate (Ref. 11). The standard model [Eqs. (3) and (4)], which does not include local effects of the adsorbates, reproduces the data quite well.

these experiments.

The experiments were performed on single crystals of Cu(100) and Cu(110), which were cleaned using standard sputter and anneal cycles. The surface long-range order was monitored using low-energy electron diffraction (LEED). Alkali-metal overlayers were deposited using thoroughly outgassed getters.[33] The surface cleanliness and the overlayer coverages were measured with Auger electron spectroscopy (AES). A Kelvin probe was used to measure changes in the work function of the sample. The clean-surface work functions were taken to be $\Phi=4.59$ eV for Cu(100) and $\Phi=4.48$ eV for Cu(110).[34,35] The observed neutralization versus work function depends slightly on the procedure used to prepare the alkali-metal overlayer. The most reproducible results were achieved for overlayers which had been briefly annealed at a moderate temperature ($\sim$200 to 400 °C).[36] Thus to achieve a desired overlayer coverage, first a high coverage was deposited. Next, the sample was annealed at a moderate temperature so that part of the overlayer thermally desorbed. This procedure was used for the experiments on Cu(100), while the overlayer was not annealed for the experiments on Cu(110).

As mentioned previously, the overlayer coverage was measured using AES. To calibrate the AES signal, we measured the work function of the sample versus the AES signal for a series of alkali-metal exposures. The coverage calibration was determined by equating the minimum in this curve to a published value.[37] Figure 3 shows the measured work function versus potassium coverage for Cu(100). We note a discrepancy between our measurement and that of Dubois *et al.*[37] for the value of the work function at the minimum (Φ_{min}). (Dubois *et al.* found $\Delta\Phi_{max}\simeq 3.7$ eV to give $\Phi_{min}\simeq 0.9$ eV, while we found $\Delta\Phi_{max}\simeq 3.0$ eV to give $\Phi_{min}\simeq 1.6$ eV. Aruga *et al.*[38] also found $\Phi_{min}\simeq 1.6$ eV.) A potential error in our coverage calibration would give a somewhat different dipole moment, p, for the adsorbed K. [The adsorbate dipole moment is an input parameter in our charge-transfer model (see Sec. V).] However, we do not expect this discrepancy to change our conclusions, since our inhomogeneous model of resonant charge transfer gives similar results for dipole moments that differ by as much as $\pm 40\%$. Furthermore, experimentally, we find that the measured ion survival probability versus work function is virtually identical for 100-eV K^+ scattered from either K/Cu(100) or Cs/Cu(110).

After depositing and annealing the overlayer, the sample is allowed to cool ($T_s\sim 60-100$ °C), and the work function is measured. Then the sample is exposed to the ion beam and, using an electrostatic analyzer, an energy spectrum for the scattered ions is obtained. The beam dose during the time required to obtain an energy spectrum is very small ($\sim 10^{14}$ particles/cm^2). As a result, sputter damage to the surface and dosing effects are not a problem. (We have experimentally verified this.) If we assume that the decrease in intensity of the scattered ions with decreasing work function is caused by resonant neutralization, then coverages of less than a tenth of a monolayer of alkali-metal atoms cause dramatic changes in the neutralization rate of the scattered ions.

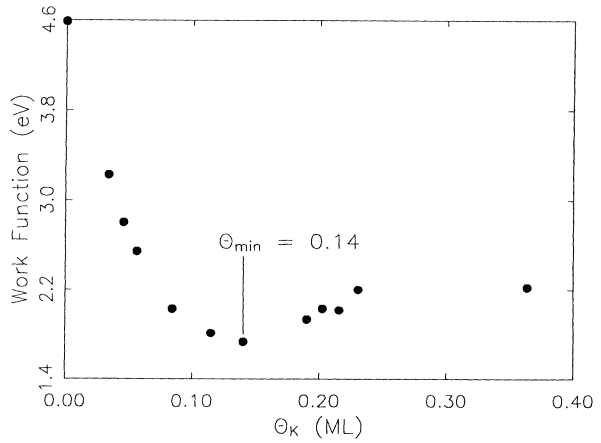

FIG. 3. Measured variation of the work function of Cu(100) vs Θ_K. Θ_K (in monolayers) is defined as the number of K atoms per Cu surface atom. The coverage was calibrated by equating the minimum in the curve with a published value (Ref. 37). The ion-scattering data presented are taken at low coverages where Φ varies linearly with K coverage.

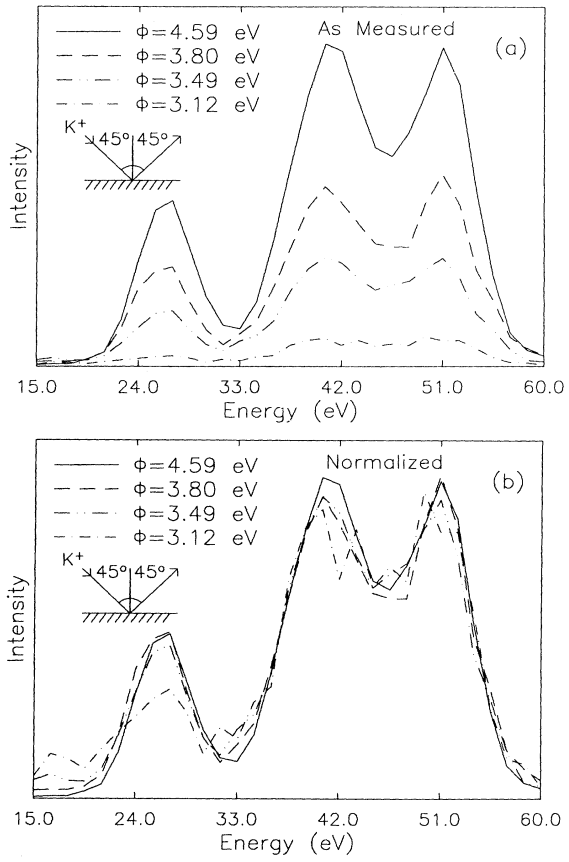

FIG. 4. Energy spectra of 100-eV K^+ scattered from clean and potassium-covered Cu(100)⟨001⟩ with $\Theta_i=\Theta_f=45°$. (a) As the work function decreases, the scattered-ion intensity decreases. (b) When normalized by the integrated intensity, the spectra look quite similar, indicating that the signal is primarily due to scattering from the copper substrate. Note also that the different peaks are all neutralized by the same amount.

IV. COMPARISON OF DATA AND STANDARD MODEL

Figure 4(a) shows a set of experimental energy spectra obtained for K^+ scattering from Cu(100) along the ⟨001⟩ azimuth. The beam was incident at an angle of 45° from the surface normal and the ions scattered at 45° (also with respect to the surface normal) were detected. The spectra are obtained from clean and potassium-covered Cu(100).

From a computer simulation of the scattering process, we can identify the types of scattering events which contribute to each of the peaks in Fig. 4(a).[26] Figure 5 shows a simulated spectrum for K^+ on Cu(100)⟨001⟩ which, like the data, has three peaks. Trajectory analysis shows that the low-, middle-, and high-energy peaks are due primarily to quasi-single- (QS) scattering, zigzag, and quasi-double- (QD) scattering events, respectively.[39]

In Fig. 4(b), we see that the energy spectra from Fig. 4(a) look quite similar when normalized by the total integrated intensity in each spectrum. In particular, we note that no new peaks are evident in the spectra for scattering from the potassium-covered surfaces, indicating that the ions detected are ones which have collided with copper substrate atoms. Figure 4(b) also shows that the intensities of the peaks decrease by the same amount for a given work function (potassium coverage), indicating that the different types of trajectories have the same ion-survival probability.[40]

Figures 6(a)–6(c) show the measured ion-survival probability for the quasi-single and quasi-double peaks as a function of work function for the data shown in Fig. 4.[41] Note that P^+ is unity for scattering from clean Cu ($\Phi=4.59$ eV), but drops to ~ 0.05 when $\sim 4\%$ of a monolayer of K is preadsorbed on the surface ($\Phi=3.1$ eV). (At such low coverages, the work function varies linearly with K coverage.) Since there is little difference in neutralization within a given spectrum for the data presented in Figs. 7–9, the ion-survival probability P^+

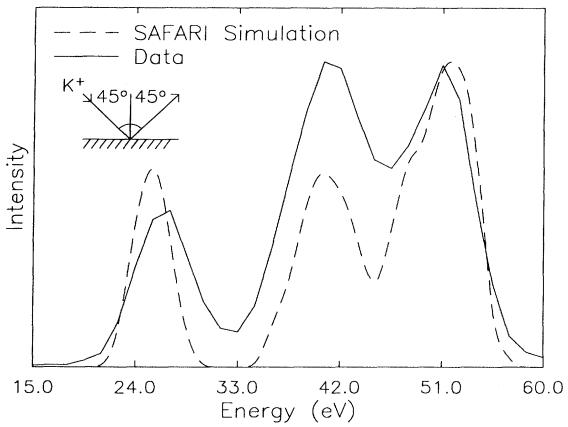

FIG. 5. Measured and simulated ion-scattering spectra for 100-eV K^+ scattered from Cu(100)⟨001⟩, $\Theta_i=\Theta_f=45°$. The computer simulation allows us to identify the types of trajectories which are observed experimentally. These trajectories are used in the model calculations of the ion survival probability (see text).

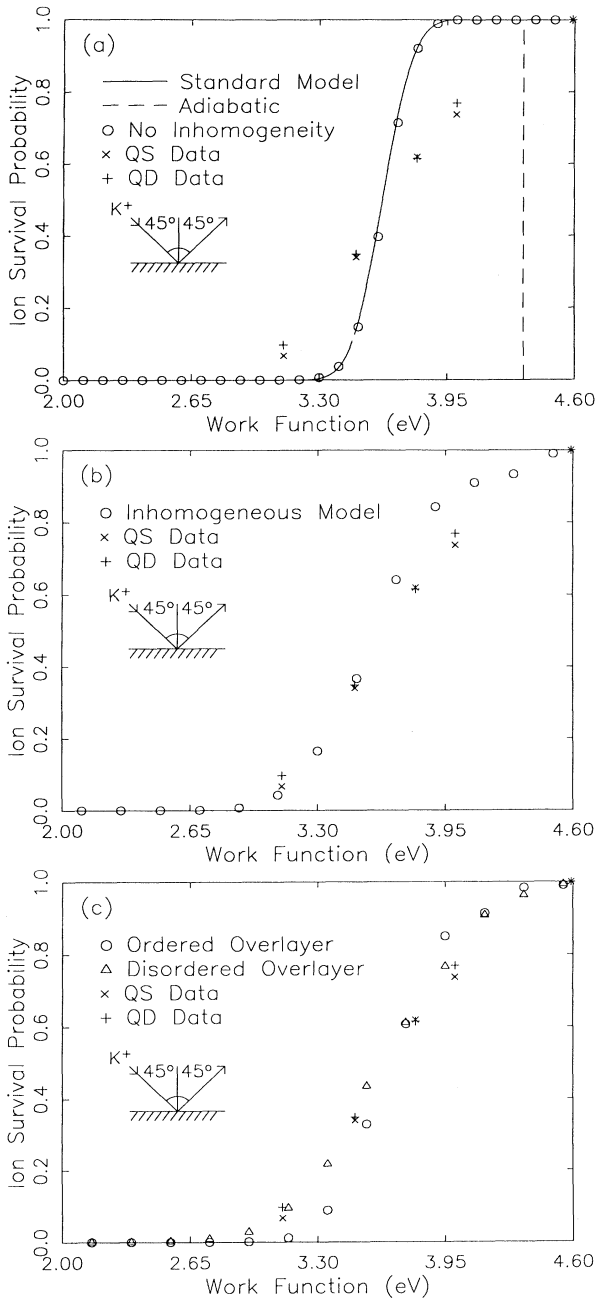

FIG. 6. Comparison of data and models for the ion survival probability of 100-eV K^+ scattered from Cu(100)⟨001⟩/K, $\Theta_i=\Theta_f=45°$. (a) The experimental values of the ion survival probability for the QS- and QD-scattering trajectories, from the data shown in Fig. 4, are quite similar. The standard model [Eqs. (3) and (4)] and our model without local effects (which agree with each other) do not reproduce the data. The ion survival probability in the adiabatic limit is also shown (dashed line). (b) Same data compared with our model, which includes the local electrostatic potential of the adsorbates. The more gradual decrease of the ion survival probability vs work function is reproduced by the model. (c) Same data compared with our model using a larger level width and two different overlayer models (see text). The calculations give qualitatively similar results, indicating that the role of the local electrostatic potential of the adsorbate overlayer is important in the charge-transfer process.

that is cited at a given work function will be the integrated intensity for the entire energy spectrum, normalized by the integrated intensity for scattering from the clean surface.

The ion-survival probabilities predicted by Eq. (4) are shown in Fig. 6(a) along with the data. The values of Δ_0 and α were taken from Nordlander's calculations for K interacting with a jellium surface ($r_s=2$).[42] Equation (4) does not reproduce the data. The measured intensity decrease with decreasing work function is more gradual than that predicted by the calculation. Even if Δ_0 and α are treated as parameters in a best fit of Eq. (4) to the data, the agreement is not satisfactory, and the resulting values of Δ_0 and α are physically unreasonable.[13]

Geerlings *et al.* found similar discrepancies for alkali metals scattered from adsorbate-covered W(110).[12] They concluded that the local adsorbate-induced electrostatic potential needed to be included in order to reconcile the experimental data with the standard model of resonant charge transfer. We have also found that this is required to explain our data. However, both the experiment and calculation differ significantly from that of Geerlings *et al.*, as described below.

V. LOCAL ADSORBATE-INDUCED EFFECTS

In the standard model, the point at which the atom-metal and ion-metal systems are degenerate (i.e., the diabatic curves cross) depends only on the distance of the atom from the surface. For the case of an adsorbate-covered surface, the energy of the scattering-particle's ionization level will also vary due to the local electrostatic potential of the adsorbates. This potential, $V_{\rm ads}(\mathbf{r})$, varies with lateral position near the surface, and approaches zero at distances large compared to the average spacing between adsorbates. Typically in our experiments, the spacing between adsorbates is large compared to the level-crossing distance. Therefore, $V_{\rm ads}(\mathbf{r})$ is not laterally homogeneous at the distances where the final charge state of the scattered ions is most likely to be determined. As a result, the level-crossing distance depends on the position of the scattering-particle's trajectory relative to nearby adsorbates.

To see how an atomic ionization level varies in the local electrostatic potential, we can imagine ionizing the atom at $z=\infty$ and then bringing the ion into some position near the surface. The first step requires an energy equal to I. The second step lowers the energy by $(1/4z)-V_{\rm ads}(\mathbf{r})$. Therefore,

$$\begin{aligned}\varepsilon_a(\mathbf{r})&=-I+\frac{1}{4(z-z_{\rm im})}-V_{\rm ads}(\mathbf{r})\\&=\varepsilon_a^0(z)-V_{\rm ads}(\mathbf{r})\ .\end{aligned}\tag{5}$$

A level crossing occurs when $\varepsilon_a(\mathbf{r}_c)=-\Phi$:

$$\varepsilon_a^0(z_c)-V_{\rm ads}(\mathbf{r}_c)=-\Phi\ .\tag{6}$$

As can be seen from Eq. (6), the ion survival probability will now depend on the position of a scattered particle with respect to the surrounding adsorbates. Furthermore, for a given scattering trajectory, more than one level crossing is possible. Equations (3) and (4), which were derived assuming $\varepsilon_a(z)$ decreased monotonically and that z_c did not depend on lateral position, are no longer appropriate.

We have therefore extended the standard model of resonant charge transfer to include the effects of the local electrostatic potential of an adsorbate layer. Our calculation uses a program which numerically integrates the solution to the time-dependent Schrödinger equation for the occupancy of the atomic level as a function of time.[43]

The starting point in this model is the spinless Anderson Hamiltonian[1,4,5]

$$H(t)=\sum_k \varepsilon_k n_k+\varepsilon_a(t)n_a+\sum_k [V_k(t)c_a^\dagger c_k+\text{H.c.}]\ ,\tag{7}$$

where ε_k and ε_a are the energies of the metal electronic levels and the atomic level, respectively. n_k and n_a are the corresponding number operators, $n_i=c_i^\dagger c_i$. V_k is $\langle a|V|k\rangle$, with V representing the coupling of the atomic state to those in the metal. The potential is assumed to introduce no coupling between the metallic levels ($V_{kk'}=0$). The atom's position is a specified function of time (the trajectory approximation), so that the atomic-level energy and coupling to the metal are both explicit functions of time.

The Hamiltonian, Eq. (7), leads to equations of motion for c_a and c_k:

$$i\frac{\partial c_a(t)}{\partial t}=\varepsilon_a(t)c_a(t)+\sum_k V_k^*(t)c_k(t)\ ,\tag{8}$$

$$i\frac{\partial c_k(t)}{\partial t}=\varepsilon_k(t)c_k(t)+V_k(t)c_a(t)\ .\tag{9}$$

To solve Eqs. (8) and (9), some simplifying assumptions are usually made; $V_k(t)$ is taken as $V_k(t)=u(t)V_k$ and

$$\Delta(\varepsilon)=\pi\sum_k |V_k|^2\delta(\varepsilon-\varepsilon_k)=\pi|V|^2\rho=\Delta_0\ .\tag{10}$$

In Eq. (10), Δ is the half-width of the atomic level, which is precisely one-half the transition rate given by Fermi's golden rule. These assumptions correspond to a surface with a wide band and a density of states that is constant in energy.[1,7] With these assumptions, the occupancy of the atomic level as a function of time, $n_a(t)$, is

$$n_a(t)=n_a(t_0)\exp\left[-2\int_{t_0}^t\Delta(t')dt'\right]+\frac{1}{\pi}\int d\varepsilon\, f(\varepsilon,T)\left|\int_{t_0}^t\sqrt{\Delta(t')}\exp\left[-i\varepsilon t'-\int_{t'}^t[i\varepsilon_a(t'')+\Delta(t'')]dt''\right]dt'\right|^2\ ,\tag{11}$$

where f is the Fermi function and $\Delta(t)=\Delta_0|u(t)|^2$. The first term arises from the decay of the initially filled level [if $n_a(t_0)=1$] into the continuum of metal states at a rate $\Delta(t)$. The role of this "memory" term has been discussed elsewhere.[4] For our ion-scattering experiments, $n_a(t_0)=0$, and the memory term is zero (i.e., the incident particle is an ion). Our simulations indicate that the final charge state of the scattered particle is independent of the

charge state and trajectory of the incident ion (i.e., the particle loses memory of the incident charge state, as discussed in Ref. 4), but this has not been tested in our experiments. The second term arises from the filling of the level by occupied metal states (states with $\varepsilon \leq E_F$). In the absence of inhomogeneities, the ion survival probability [Eq. (3)] is simply given by $1-n_a(\infty)$ [from Eq. (11)].

We will discuss our calculation including the inhomogeneities for the case of K^+ scattering from K/Cu(100). The energy of the atomic level [K (4*s*)], $\varepsilon_a(t)$, and the coupling $\Delta(t)$ are found as follows. At the distances of interest in our experiment, the dipole moment will be the dominant term in a multipole expansion of the adsorbate's true electrostatic potential. Therefore, as in a previous study,[12] the adsorbate overlayer $V_{\rm ads}(\mathbf{r})$ is modeled as an array of dipoles. The dipole moment p of K adsorbed on Cu(100) is determined from the initial slope of our measurement of the work function versus coverage (Fig. 3). The experimental value $p=2.64$ (atomic units) compares well with other experimental values and the results of calculations by Lang.[44] The density of dipoles is determined from the measured work-function shift.

Various arrangements of the adsorbates (e.g., ordered, disordered, etc.) can be used in the simulation. The method of calculating the electrostatic potential of the adsorbate layer depended on the type of overlayer. In all cases, the convergence of the calculation was checked. For the ordered overlayers, the potential was calculated using Fourier transforms on an infinite array. Enough terms in the **k**-space expansion were kept to insure convergence. The disordered overlayers were represented by an array of discrete dipoles within a large circle (radius $=R$) and an infinite electrostatic double layer outside of this circle. The total electrostatic potential was found by directly summing the potential of the individual adsorbates and then adding the contribution from the double layer. The radius R was large enough so that the results were independent of R.

A scattering trajectory generated by the program SAFARI gives the position of the particle as function of time, $\mathbf{r}(t)$. $V_{\rm ads}(\mathbf{r})$ and $\mathbf{r}(t)$ are used in Eq. (5) to find $\varepsilon_a(\mathbf{r}(t))$, which is then used in Eq. (11) to find the occupancy of the level as a function of time. We assume the presence of the adsorbates does not change the coupling of the atomic and metallic states or the scattering trajectory. Therefore, $\Delta(t)$ is determined using $\Delta(t)=\Delta(z(t))=\Delta_0 e^{-\alpha z(t)}$ and is not a function of lateral position on the surface.[45] The ion survival probability P^+ for a given trajectory is $1-n_a(\infty)$ [from Eq. (11)]. [In our calculation, P^+ is actually determined from a time-evolution operator solution of Eqs. (8) and (9), which is more amenable to numerical solution than Eq. (11).[43]]

At low coverages and room temperature, we do not expect any particular registry of adsorbates on the Cu(100) surface. Thus, to simulate the scattering experiment, we calculate P^+ for a number of trajectories (several hundred typically) which are randomly displaced with respect to the adsorbate overlayer. The final probability is the average of these. The simulation is repeated for several different adsorbate coverages (i.e., dipole arrays with different spacings). In this way, the ion-survival probability versus work function is calculated.

Figure 6(b) shows the results of this calculation where Δ_0 and α were the same as those used in Fig. 6(a). The calculation reproduces the data quite well. In particular, a slow transition from no neutralization to almost complete neutralization is observed.

The magnitude of the coupling between the atomic state and the metallic states is difficult to calculate and subject to some uncertainty.[46] The values for Δ_0 and α which we have used are, as mentioned above, taken from a calculation by Nordlander and Tully for K interacting with jellium ($r_s=2$) and should only be viewed as an estimate of the magnitude of the coupling. As a result, we also used values of Δ_0 that were one half and twice as large as the theoretical values. Figure 6(c) demonstrates the effect of increasing the level width by a factor of 2. Two calculations with the inhomogeneous model, using an ordered overlayer (square lattice) and a disordered overlayer with adsorbate-adsorbate repulsion, are compared in Fig. 6(c). For the disordered overlayer, we assumed the adsorbate-adsorbate interaction to be given by the electrostatic interaction of two dipoles. The adsorbates (dipoles) where then randomly distributed on the surface, with the restriction that the minimum distance allowed between adsorbates was the distance at which the energy of interaction was equal to the thermal energy of the adsorbates. The results are qualitatively similar to those in Fig. 6(b). As might be expected, the disordered overlayer reproduces the data slightly better than the ordered overlayer. The calculations shown in Figs. 6(b) and 6(c) use a quasi-single-scattering trajectory. Calculations using other types of scattering trajectories (e.g., quasi-double scattering) also give qualitatively similar results. However, when the local electrostatic potential of the overlayer is not included, no values of Δ_0 and α can be found which bring the theory into agreement with the data. In Fig. 6(a) we show results from our calculation where the inhomogeneity $V_{\rm ads}(\mathbf{r})$ was set equal to zero, giving P^+ values that are equivalent to those calculated from Eq. (4). This leads us to conclude that in our experiments the local electrostatic potential plays a crucial role in the resonant charge-transfer process.

A number of assumptions are made implicitly in our model of the experimental results. The first is that the observed neutralization is due to resonant charge transfer rather than some other process, such as Auger. It is generally assumed that resonant charge transfer will be the dominant neutralization process for electron transfer to levels lying near the Fermi level (as in the case for scattered alkali-metal atoms).[4] This calculation also neglects spin effects and the filling of multiple levels (e.g., filling of the affinity level[47–49]) in the scattered potassium. However, for the work functions and scattered-K velocities of interest here, we do not expect this to change the calculated P^+ values by more than a few percent.[50] In addition to these more general assumptions, we have also assumed that Δ depends only on z and that the adsorbates have no effect on the scattering trajectories. Because the density of adsorbates is so low for the work functions of interest (see Fig. 3), very few of the incident ions scatter

from adsorbates.[51] (The scattering cross section at the energies in our experiments is much smaller than the range over which adsorbates influence charge transfer.) The model also ignores the effect of any electronic excitations in the metal caused by the collision of the atom with the surface. If excited electrons in the metal were playing an important role in the charge transfer, we might expect to see neutralization for K^+ scattered from clean Cu(100). We have recently installed a detector for neutral alkalis in our system and we find no neutralization for 100-eV K^+ scattered from clean Cu(100). Furthermore, Algra *et al.* found essentially no neutralization of 2–10-keV K^+ scattered from clean Cu(100).[9] We have also neglected the possibility that the scattered ion might cause some depolarization of a nearby adsorbate, thereby changing the effective dipole moment of the adsorbate.

VI. FURTHER DISCUSSION AND TESTS OF THE INHOMOGENEOUS MODEL

In the standard model, the neutralization of scattered particles is a sensitive function of the perpendicular velocity v_z [Eqs. (3) and (4)]. This can be tested experimentally by changing the beam energy and scattering geometry. Figure 7 shows the measured ion survival probabilities for K^+ scattering from Cs/Cu(110) along the $\langle 1\bar{1}0 \rangle$ azimuth.[13] The scattering geometry is the same in each case and the incident energies are 100, 400, and 1000 eV. The data do not show the velocity dependence expected from Eqs. (3) and (4), as can be seen more clearly in Fig. 8, where the ion survival probability is plotted on a logarithmic scale. Also plotted in Fig. 8 are the predictions of the ion survival probability using Eq. (4) and using our inhomogeneous-model calculation. For the inhomogeneous-model calculations, we used an ordered overlayer with a level width twice as large as the Nordlander and Tully calculation, with a dipole moment and coverages appropriate for Cs adsorbates and with the work function for Cu(110) (4.48 eV).[34,35] At small work functions, the standard model predicts, for a given work function, a substantial difference in the 100-, 400-, and 1000-eV ion survival probabilities, which is not seen in the data. We believe that the velocity dependence predicted by the standard model is obscured by the averaging of the total ion survival probability over all the individual ion trajectories that sample the inhomogenous electrostatic potential of the adsorbates. When the effects of the adsorbates are included in the calculation, the velocity dependence seen in the data is reproduced.

Although the velocity dependence predicted by the standard model is not observed in the data or our calcula-

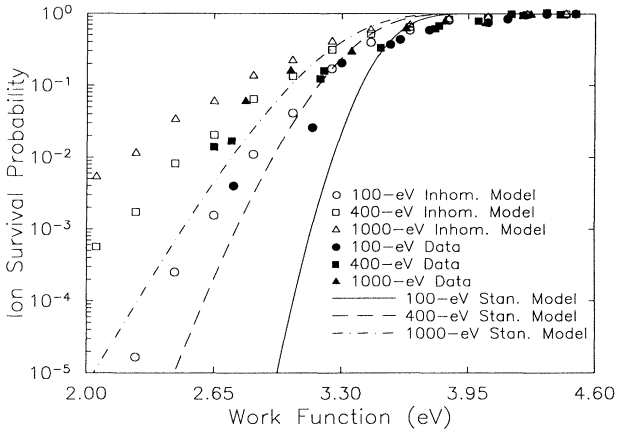

FIG. 8. The data from Fig. 7 plotted on a logarithmic scale along with the standard model [Eqs. (3) and (4)] and our calculations. In the standard model, the ion survival probability is very sensitive to the perpendicular velocity of the scattered particles (particularly at small work functions). The data do not show this dependence. The model which includes the inhomogeneities reproduces the velocity dependence seen in the data.

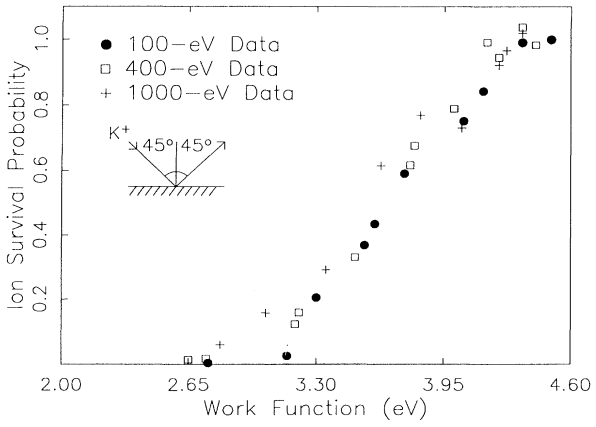

FIG. 7. Ion survival probabilities for 100-, 400-, and 1000-eV K^+ scattered from Cs/Cu(110)$\langle 1\bar{1}0 \rangle$, $\Theta_i = \Theta_f = 45°$. The observed ion survival probability is not very sensitive to the incident energy.

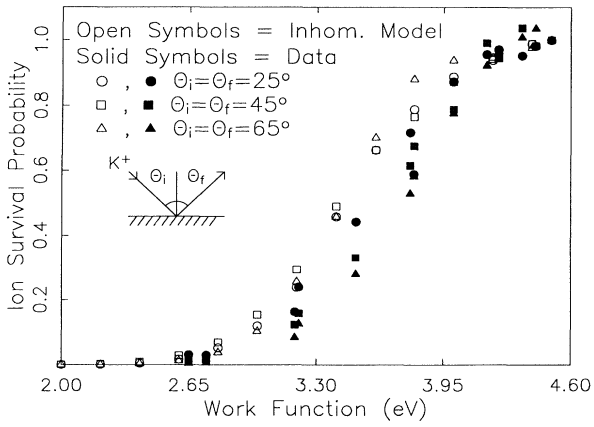

FIG. 9. Comparisons of measured and calculated ion survival probabilities for 400-eV K^+ scattered from Cs/Cu(110)$\langle 1\bar{1}0 \rangle$ for three different scattering geometries: $\Theta_i = \Theta_f = 25°$, 45°, and 65° from normal.

tions, the ion survival probability depends on the velocity of the ion normal to the surface, since the coupling Δ of the atomic level to the metallic states is still assumed to depend only on the distance of the atom from the surface. If lateral variations in the coupling of the atomic state to the surface states were included in the model, the ion survival probability would no longer have a simple dependence on the perpendicular velocity of the atom.

Figure 9 shows the measured ion survival probabilities for 400-eV K^+ scattering from Cu(110)$\langle 1\bar{1}0\rangle$/Cs for three different scattering geometries. Because of differing collisional energy losses for the different scattering geometries, these three cases all have very similar perpendicular velocities, but very different parallel velocities. Figure 9 also shows the results of our model for these cases. As expected, the model predicts very small differences for the different scattering geometries.

We conclude this section with a brief comparison of our conclusions with those of published experiments. The first is with the results of Geerlings *et al.*, who measured the ion survival probabilities for Li, K, and Cs scattered from W(110)/Cs.[12] Their analysis was performed for Cs scattering. Because of the scattering geometries and Cs adsorbate coverages for that experiment, they concluded that all the scattered Cs particles which were detected had collided with Cs adsorbates. In contrast, trajectory analysis indicates that in our experiment the ions detected have scattered from the Cu substrate atoms, and we assume that the incident ions are randomly located with respect to the adsorbates. The analysis of Geerlings *et al.* differs from ours in the magnitudes of the couplings Δ they have used and their use of a component of velocity perpendicular to a seam that represents an equipotential surface of the adsorbate overlayer. In our calculation, since we solve for the ion survival probability in the time domain [Eq. (5)], we make no assumptions about velocity components. We do assume that Δ depends only on z, as do Geerlings *et al.* Because of the differences in both the experiments and the models, specifics of the interpretation of the results are quite different in the two cases. However, both their experiment and ours indicate that the local inhomogeneities in the electrostatic potential of the adsorbate layer can be important in the charge-transfer process for scattered alkali-metal atoms.

Our model of the resonant charge-transfer process suggests some reasons why the data from Yu's sputtering experiment[11] (Fig. 2) agrees with Eq. (4), which ignores lateral variations in the local electrostatic potential. First, in that experiment, different coverages of Li coadsorbed with Cs are used to induce the work-function shift. The dipole moment of Li is considerably smaller than that of Cs or K and thus a higher coverage of Li is required to produce a comparable work-function shift. Since the lateral inhomogeneities of the adsorbate-induced potential decrease as the adsorbate coverage increases, the standard model becomes a better approximation. Second, before the Cs atom is sputtered from the surface, it is not likely to be near another adsorbate (Li or Cs) due to the repulsion between adsorbates. This may lead to selective sampling of the laterally inhomogeneous potential as the sputtered particle leaves the surface, as opposed to the random sampling in scattering experiments. We have done simulations suggesting that both mechanisms may influence the results.

VII. CONCLUSIONS

We have measured ion survival probabilities for K^+ scattered from adsorbate-covered Cu(100) and Cu(110). We find that a model of resonant charge transfer based on the spinless Newns-Anderson Hamiltonian adequately explains our data so long as the local elecrostatic potential of the adsorbate overlayer is included in the calculations. In modeling the data, we used realistic ion-scattering trajectories generated by SAFARI and a dipole model of the adsorbate overlayer. The parameters used in the model were either experimentally determined or taken from theoretical calculations.

The results of the model indicate that, because of the locally varying electrostatic potential around adsorbate sites, those ions which scatter near an alkali-metal adsorbate are more likely to be neutralized than those which scatter far from an adsorbate. Since the ion-scattering experiments sample a macroscopic region of the surface, the experimentally measured ion survival probabilities are an average of the local-ion survival probabilities. This averaging process causes the gradual decrease in the ion survival probability as the work function decreases. It also masks the expected velocity dependence predicted by the standard model [Eq. (3)].

ACKNOWLEDGMENTS

We would like to thank Alan Dorsey, Karsten Jacobsen, and Brad Marston for their input into the calculations used in this paper, and Peter Nordlander for supplying us with results of alkali-metal level energy and width calculations prior to publication. We would also like to acknowledge several helpful and stimulating discussions with Jim Sethna, John Wilkins, Dennis Newns, Norton Lang, John Harris, Bengt Kasemo, Stephen Holloway, and Jens Nørskov. This work was supported by the National Science Foundation (NSF) (Grant Nos. DMR-PYI-8451979 and DMR-8821846) and the Air Force Office of Scientific Research (AFOSR) (Grant No. 88-0069). Calculations were performed at the Cornell Theory Center and the Cornell Materials Science Center computing facility.

*Present address: IBM Thomas J. Watson Research Center, P.O. Box 218, Yorktown Heights, NY 10598.

†Present address: Department of Physics, The Ohio State University, Columbus, OH 43210-1106.

[1] A. Blandin, A. Nourtier, and D. W. Hone, J. Phys. (Paris) **37**, 369 (1976).

[2] J. C. Tully, Phys. Rev. B **16**, 4324 (1977).

[3] J. K. Nørskov and B. J. Lundqvist, Phys. Rev. B **19**, 5661

(1979).
[4]R. Brako and D. M. Newns, Surf. Sci. **108**, 253 (1981).
[5]N. D. Lang, Phys. Rev. B **27**, 2019 (1983).
[6]N. D. Lang and J. K. Nørskov, Phys. Scr. **T6**, 15 (1983).
[7]D. M. Newns, K. Makohsi, R. Brako, and J. N. M. van Wunnik, Phys. Scr. **T6**, 5 (1983).
[8]N. D. Lang, J. K. Nørskov, and B. I. Lundqvist, Phys. Scr. **34**, 77 (1986).
[9]A. J. Algra, E. v. Loenen, E. P. Th. M. Suurmeijer, and A. L. Boers, Radiat. Eff. **60**, 173 (1982).
[10]M. L. Yu, Phys. Rev. Lett. **40**, 574 (1978).
[11]M. L. Yu and N. D. Lang, Phys. Rev. Lett. **50**, 127 (1983).
[12]J. J. C. Geerlings, L. F. Tz. Kwakman, and J. Los, Surf. Sci. **184**, 305 (1987).
[13]G. A. Kimmel, D. M. Goodstein, and B. H. Cooper, J. Vac. Sci. Technol. A **7**, 2186 (1989).
[14]P. Nordlander, Scanning Electron Microsc. S **4**, 353 (1990).
[15]J. Los and J. J. C. Geerlings, Phys. Rep. **190**, 133 (1990).
[16]R. Brako and D. M. Newns, Rep. Prog. Phys. **52**, 655 (1989).
[17]P. Sjövall, B. Hellsing, K.-E. Keck, and B. Kasemo, J. Vac. Sci. Technol. A **7**, 1065 (1987).
[18]J. K. Nørskov, S. Holloway, and N. D. Lang, Surf. Sci. **137**, 65 (1984).
[19]N. D. Lang, S. Holloway, and J. K. Nørskov, Surf. Sci. **150**, 24 (1985).
[20]K. Markert and K. Wandelt, Surf. Sci. **159**, 24 (1985).
[21]H. D. Hagstrum, Phys. Rev. Lett. **43**, 1050 (1979).
[22]H. Conrad, G. Ertl, J. Kuppers, S. W. Wang, K. Gerhard, and H. Haberland, Phys. Rev. Lett. **42**, 1082 (1979).
[23]J. Lee, C. Hanrahan, J. Arias, F. Bozso, R. M. Martin, and H. Metiu, Phys. Rev. Lett. **54**, 1440 (1985).
[24]B. Woratschek, W. Sesselmann, J. Kuppers, G. Ertl, and H. Haberland, Phys. Rev. Lett. **55**, 1231 (1985).
[25]J. J. C. Geerlings and J. Los, Phys. Lett. **102A**, 204 (1984).
[26]D. M. Goodstein, S. A. Langer, and B.H. Cooper, J. Vac. Sci. Technol. A **6**, 703 (1988).
[27]R. W. Gurney, Phys. Rev. **47**, 479 (1935).
[28]J. W. Gadzuk, Surf. Sci. **6**, 133 (1967).
[29]The image interaction is the main interaction at the distances at which charge transfer is important. Closer to the surface, the representation of the interaction by the image potential is no longer valid.
[30]N. D. Lang, and W. Kohn, Phys. Rev. B **7**, 3541 (1973).
[31]Therefore, instead of having just two diabatic curves as in Fig. 1(a), there is a manifold of curves corresponding to all combinations of electron-hole pair excitations in the metal.
[32]R. L. McEachern, D. L. Adler, D. M. Goodstein, G. A. Kimmel, B. R. Litt, D. R. Peale, and B. H. Cooper, Rev. Sci. Instrum. **59**, 2560 (1988).
[33]SAES Getters/USA Inc., Colorado Springs, CO.
[34]H. B. Michaelson, J. Appl. Phys. **48**, 4729 (1977).
[35]P. O. Gartland, Phys. Norv. **6**, 201 (1972); P. O. Gartland, S. Berge, and B. J. Slagsvold, Phys. Norv. **7**, 39 (1973).
[36]H. D. Hagstrum, P. Petrie, and E. E. Chaban, Phys. Rev. B **38**, 10264 (1988).
[37]L. H. Dubois, B. R. Zegarski, and H. S. Luftman, J. Chem. Phys. **87**, 1367 (1987).
[38]T. Aruga, H. Tochihara, and Y. Murata, Phys. Rev. B **34**, 8237 (1986).
[39]In a quasi-single collision, the scattered ion transfers momentum primarily to one surface atom. In a quasi-double collision, the scattered ion transfers momentum primarily to two surface atoms. The discrepancies in peak heights between the simulation and the data are due to details of the scattering potential which are of no interest here.
[40]The QS- and QD-scattering trajectories have different final velocities, but the difference in neutralization based on the standard model is expected to be small (see Fig. 2, Ref. 13), as is seen in the data.
[41]The ion survival probabilities for the quasi-single and quasi-double peaks were found by integrating the intensity within a small range in energy centered on the respective peaks (Fig. 4) and then normalizing by the clean surface intensity.
[42]P. Nordlander and J. C. Tully, Surf. Sci. **211/212**, 207 (1989).
[43]A. T. Dorsey, K. W. Jacobsen, Z. H. Levine, and J. W. Wilkins, Phys. Rev. B **40**, 3417 (1989).
[44]See, N. D. Lang, Phys. Rev. B **4**, 4234 (1971), and references therein.
[45]Peter Nordlander also gave us the results of his calculation of the level widths versus distance, and we used these directly in some of our calculations instead of fitting to an exponential form. The results were very similar for both treatments of the level width.
[46]D. M. Newns, Comm. Condens. Matter Phys. **14**, 295 (1989).
[47]H. Kasai and A. Okiji, Surf. Sci. **183**, 147 (1987).
[48]H. Nakanishi, H. Kasai, and A. Okiji, Surf. Sci. **197**, 515 (1988).
[49]K. W. Sulston, A. T. Amos, and S. G. Davison, Phys. Rev. B **37**, 9121 (1988).
[50]We have compared the Brako-Newns calculations [Eq. (4)] with the results of a more complete theory, based on a variational expansion in particle-hole pairs, that includes negative ions and electron spin. The positive-ion yields agree well over the range of velocities and work functions that we consider here. The Brako-Newns calculation typically overestimates P^+ by less than 5%. Also, the predicted negative-ion yield is extremely small ($P^- \ll 0.1\%$) for work functions greater than 2.3 eV (J. B. Marston, private communication).
[51]Using SAFARI, we performed Monte Carlo simulations of scattering from an adsorbate-covered surface and found only small changes in the scattering spectra due to scattering from the adsorbates. We did not consider the effect of the adsorbate dipole field on the scattering trajectories.